



HAL
open science

Intracellular AIEC LF82 relies on SOS and stringent responses to survive, multiply and tolerate antibiotics

Gaëlle Demarre, Victoria Prudent, Hanna Schenk, Emilie Rousseau,
Marie-Agnès Bringer, Nicolas Barnich, Guy Tran van Nhieu, Sylvie Rimsky,
Silvia de Monte

► To cite this version:

Gaëlle Demarre, Victoria Prudent, Hanna Schenk, Emilie Rousseau, Marie-Agnès Bringer, et al..
Intracellular AIEC LF82 relies on SOS and stringent responses to survive, multiply and tolerate
antibiotics. 2019. hal-02789654

HAL Id: hal-02789654

<https://hal.inrae.fr/hal-02789654>

Preprint submitted on 5 Jun 2020

HAL is a multi-disciplinary open access archive for the deposit and dissemination of scientific research documents, whether they are published or not. The documents may come from teaching and research institutions in France or abroad, or from public or private research centers.

L'archive ouverte pluridisciplinaire **HAL**, est destinée au dépôt et à la diffusion de documents scientifiques de niveau recherche, publiés ou non, émanant des établissements d'enseignement et de recherche français ou étrangers, des laboratoires publics ou privés.



Distributed under a Creative Commons Attribution - NonCommercial - NoDerivatives 4.0
International License

1 Intracellular AIEC LF82 relies on SOS and stringent responses to survive, multiply and
2 tolerate antibiotics.

3

4 Gaëlle Demarre ^{1,2}, Victoria Prudent ¹, Hanna Schenk ³, Emilie Rousseau ¹, Marie-Agnes
5 Bringer ^{5,6}, Nicolas Barnich ⁶, Guy Tran Van Nhieu ¹, Sylvie Rimsky ¹, Silvia De Monte ^{3,6}
6 and Olivier Espéli ^{1,*}.

7

8 Affiliations

9 ¹ CIRB – Collège de France, CNRS-UMR724, INSERM U1050, PSL Research University, 11
10 place Marcelin Berthelot 75005 Paris, France.

11 ² Inovarion, Paris, France

12 ³ Department of Evolutionary Theory, Max Planck Institute for Evolutionary
13 Biology, Plön, Germany

14 ⁴ Centre des Sciences du Goût et de l'Alimentation, 21000 Dijon

15 ⁵ Microbes, Intestin, Inflammation et Susceptibilité de l'Hôte. UMR Inserm/ Université
16 d'Auvergne U1071, USC INRA 2018

17 ⁶ Institut de Biologie de l'Ecole Normale Supérieure, Département de Biologie, Ecole
18 Normale Supérieure, CNRS, INSERM, PSL Research University, Paris, France

19

20

21 * for correspondence: olivier.espeli@college-de-france.fr

22

23

24

25 **Abstract**

26 Adherent Invasive *Escherichia coli* (AIEC) strains recovered from Crohn's disease lesions
27 survive and multiply within macrophages. A reference strain for this family, AIEC LF82,
28 forms microcolonies within phagolysosomes, an environment that prevents commensal
29 *E. coli* multiplication. Little is known about the LF82 intracellular growth status, and
30 signals leading to macrophage intra-vacuolar multiplication. We used single-cell
31 analysis, genetic dissection and mathematical models to monitor the growth status and
32 cell cycle regulation of intracellular LF82. We found that within macrophages, bacteria
33 may replicate or undergo non-growing phenotypic switches. This switch results from
34 stringent response firing immediately after uptake by macrophages or at later stages,
35 following genotoxic damage and SOS induction during intracellular replication.
36 Importantly, non-growers resist treatment with various antibiotics. Thus, intracellular
37 challenges induce AIEC LF82 phenotypic heterogeneity and non-growing bacteria that
38 could provide a reservoir for antibiotic-tolerant bacteria responsible for relapsing
39 infections.

40

41 **Introduction**

42 Adherent Invasive *Escherichia coli* (AIEC) strains recovered from Crohn's disease (CD)
43 lesions are able to adhere to and invade cultured intestinal epithelial cells and to survive
44 and multiply within macrophages (Glasser et al 2001). Attention around the potential
45 role of AIEC in the pathophysiology of CD is growing (Elhenawy *et al*, 2018); however
46 much remains to be learned about the host-pathogen interactions that govern AIEC
47 infection biology. The diversity of virulence factors displayed by multiple AIEC strains
48 suggests that members of this pathovar have evolved different strategies to colonize
49 their hosts. AIEC ability to persist, and in some cases replicate within macrophages is
50 particularly intriguing. Previous work performed with murine macrophage cell lines has
51 revealed that LF82, the first AIEC to have been characterized, multiplies in a vacuole
52 presenting the characteristics of a mature phagolysosome (Bringer *et al.*, 2006). In such
53 an environment, AIEC should encounter acidic, oxidative, genotoxic and proteic stresses.
54 Screening of genes involved in LF82 fitness within macrophage has revealed that HtrA,
55 DsbA, or Fis proteins are required for optimum fitness, (Bringer *et al.*, 2005; Bringer *et*
56 *al.*, 2007; Miquel *et al.*, 2010). These observations confirmed that LF82 encounter
57 stresses in the phagolysosomes. The impact of these stresses on the survival and growth
58 of LF82 inside phagolysosomes has not yet been investigated.

59 Studies on the bacterial cell cycle of few model organisms under well-controlled
60 laboratory conditions have revealed that to achieve accurate transmission of the genetic
61 information and optimal growth of the population, molecular processes must be
62 coordinated. (for reviews see Hajduk *et al.*, 2016; Haeusser & Levin, 2008; Margolin &
63 Bernander, 2004). When growth conditions deteriorate, the cell cycle can be modified
64 slightly, as in the case of cell filamentation when genotoxic stress induces the SOS
65 response, or more drastically when sporulation is induced by nutrient deprivation
66 (Jonas, 2014). Such cell cycle alterations affect the entire population. However, under
67 unperturbed conditions, a subset of the population also appears to present a
68 significantly reduced growth rate that allows tolerance to antibiotic treatments. This
69 small portion of the population, typically 1/10000 bacteria, is known as persisters
70 (Wood *et al.*, 2013; Lewis, 2010; Bigger, 1944). Persisters have been detected for a
71 number of bacteria. They can be found spontaneously in normally growing or stationary
72 phase populations, or they are induced by exogeneous stresses or mutations. Recently,
73 significant increase of the proportion of *S. typhimurium* persisters has been observed

74 when these bacteria invade macrophages (Helaine *et al.*, 2014). Using a fluorescent
75 reporter, it has been demonstrated that these persisters were not multiplying prior to
76 antibiotic addition. The same tool also revealed the presence of non-growing
77 mycobacteria inside macrophages (Mouton *et al.*, 2016). Several mediators of
78 persistence have been identified, with toxin-antitoxin modules emerging as key players
79 and the reduction of metabolic activities as the main driver of persistence (Rycroft *et al.*,
80 2018; Dörr *et al.*, 2009; Shan *et al.*, 2017; Balaban *et al.*, 2004; Harms *et al.*, 2017; Amato
81 *et al.*, 2014). Persisters are increasingly viewed as a major cause of the recurrence of
82 chronic infectious disease and could be an important factor in the emergence of
83 antibiotic resistance (Verstraeten *et al.*, 2016). In addition to persisters, bacterial
84 tolerance to antibiotic treatments has been observed. In contrast to persisters, tolerance
85 concerns the entire population. Tolerance corresponds to a weaker ability of antibiotics
86 to kill slow growing compared to fast growing bacteria. Tolerant bacteria emerge, for
87 example, in the presence of a nutritional limitation. The viability of tolerant bacteria is
88 impacted by the concentration and length of the antibiotic challenge (Kim & Wood,
89 2017). Tolerant cells have some aspect of active metabolism, and their frequency in the
90 population changes when bacterial environmental sensing is altered (Amato &
91 Brynildsen, 2015; Bernier *et al.*, 2013; Radzikowski *et al.*, 2016). Persistence is often
92 viewed as the result of a phenotypic switch ensuring long-term adaptation to variable
93 environments, however the origin of persistence and tolerance *in vivo* remain unclear,
94 and their distinction in the context of a host- pathogen interaction is difficult (Kim &
95 Wood, 2017).

96
97 In the present work, we analyzed growth characteristics of LF82 in THP1 monocytes
98 differentiated into macrophages. We observed that stresses within macrophages induce
99 a profound bacterial response that leads to the formation of non-growing and antibiotic-
100 tolerant LF82 at a high rate through the successive induction of stringent and SOS
101 responses. A portion of non-growing LF82 formed within macrophages is tolerant to
102 antibiotics and present a survival advantage. Our work revealed that internalization
103 within phagolysosomes curbs bacterial multiplication, and frequent escape from the
104 replicative cycle toward non-growing state(s) is a way to improve long-term survival in
105 the host.

106

107 **Results**

108

109 **Inside macrophages, LF82 population size increases despite extensive death.**

110 We used THP1 monocyte-derived into macrophages to monitor the population size of
111 AIEC LF82 bacteria over a 24 h period post infection (P.I.) (Figure 1A). CFU
112 measurements revealed that the LF82 population exponentially increased for 10-14
113 hours ($\tau = 0.15 \text{ h}^{-1}$, 0.21 doubling / h) after a long lag. The population reached a
114 maximum at 18-20 h of approximately 5-fold the value at 1 h; the number of LF82 then
115 slightly decreased (reaching 3 -fold) at 24 h. In this environment LF82 might
116 simultaneously encounter acidic pH, oxidative and genotoxic stresses, toxic molecules
117 such as cathepsins and a lack of important nutrients. Surprisingly, the tolerance level of
118 LF82 to any individual stress did not differ from a commensal K12 *E. coli* in *in vitro*
119 conditions (Supplementary Figure S1A). Using direct ex vivo Live and Dead labeling, it
120 has been previously proposed that LF82 are not killed or only rarely killed by
121 macrophages (Lapaquette *et al.*, 2012). We observed that this method underestimates
122 dead bacteria inside macrophages compared to the labeling dead bacteria with
123 propidium iodide (PI) immediately after macrophage lysis (Supplementary Figure S2A).
124 We observed 20 - 30% PI-positive bacteria at 1 h, 12 h, 18h and 24 h post-infection
125 (Figure 1A). To estimate the speed of dead bacteria disappearing in macrophages, we
126 observed the elimination of heat-killed bacteria by THP1 macrophages. Dead LF82
127 disappeared exponentially with a decay rate of 0.6 h^{-1} and a half-life of 1.4 h
128 (Supplementary Figure S2B); therefore dead LF82 observed at 12h, 18h or 24 h did not
129 correspond to the accumulation over infection period but rather to the bacteria killed in
130 the last 3 hours before observations. This finding led to consider that LF82 must be
131 under stress attack by macrophages at all times during infection.

132

133 **LF82 is under attack by macrophages.**

134 Using RT-qPCR, we measured the expression of genes induced by the acid response (*asr*,
135 *ydeO* and *frc*), the oxidative response (*soxS*, *ykgB*), the SOS response (*sulA*), the response
136 to membrane alteration (*pspB*), the lack of Mg²⁺ (*mgrB*), the lack of phosphate (*phoB*),
137 general efflux pump (*emrK*) and the *gltT* tRNA gene that is repressed by the stringent
138 response (Figure 1B). Every response pathway was induced inside the macrophage. The
139 induction of acid and the oxidative response were already high at 1 h post-infection,

140 while the SOS response, the response to membrane alterations and to the lack of Mg²⁺,
141 were peaking at 6 h post-infection. The expression of the *gltT* tRNA is strongly repressed
142 at time point 1h indicating that stringent response is on early in the infection. The
143 induction of most pathways decreased at 24 h.

144

145 **Environmental stresses influence LF82 survival.**

146 To test the impact of stress responses on the ability of LF82 to colonize macrophage, we
147 constructed deletion mutants of several key regulators of *E. coli* stress pathways and
148 analyzed their survival. Deletion of the acid stress regulators *evgA-evgS*, *phoP* and *ydeO*
149 significantly impacted the ability of LF82 to survive and multiply within macrophages to
150 a level comparable to or even below that of a commensal K12 *E. coli* (Figure 1C). Similar
151 observations were obtained with the *rpoS* deletion (general stress response), *recA*
152 deletion (SOS response), *soxS* deletion (oxidative stress) and *pspA* and *htrA* deletions
153 (envelope damages). The ppGpp0 strain (*relA spoT* deletions) is the most impacted
154 strain; less than 5% of the initial population survived a 24 h period within macrophages.

155

156 **SOS and stringent responses severely impacted LF82 survival**

157 We explored the stringent and SOS responses in more details. RecA is the main inducer
158 of the SOS response, which activates nearly 100 genes involved in DNA repair and many
159 others with unrelated or unknown functions, but it is also a crucial to correct DNA
160 lesions by homologous recombination and translesion synthesis (Kreuzer, 2013). In
161 addition to *recA* deletion, we constructed deletions of *sula* (division inhibitor) and a
162 mutation in *lexA* (*lexAind-*), which blocks SOS induction in K12 *E. coli* and reduces
163 viability in the presence of mitomycin C for LF82 and K12 (Supplementary Figure S3A).
164 We observed that the deletion of each SOS gene significantly decreased the survival of
165 LF82 within macrophages (Figure 1C). Inside the macrophage, survival of the ppGpp0
166 strain was dramatically impacted. However, this mutant also presented a strong growth
167 defect in liquid culture that complicates interpretation of the macrophage results. To
168 study the impact of the stringent response on LF82 survival and induced antibiotic
169 tolerance, we constructed deletion mutants that might have partial stringent response
170 phenotypes; deletion of *dksA*, encoding a protein linking the stringent response to
171 transcription (Sharma & Chatterji, 2010); and deletion of the polyphosphate kinase and
172 exopolyphosphatase *ppk* and *ppx* (Rao & Kornberg, 1999). As expected, the *dksA* and

173 *ppk-ppx* deletions had a much less dramatic effect on LF82 growth and survival within
174 macrophages than the *relA-spoT* mutant; nevertheless, the *dksA* mutation significantly
175 impacted the number of live bacteria recovered at 24 h P.I. (Figure 1C). We probed the
176 ability of LF82 to survive within macrophages when both stringent and SOS responses
177 were altered. We chose to combine *dksA* deletion with *recA* deletion or *lexA*ind-
178 mutation. These strains presented a survival defect (CFU 24 h / CFU 1 h) comparable to
179 that of the single *dksA* mutant (Figure 1C). These observations demonstrate that
180 surviving LF82 simultaneously or successively require SOS and stringent responses.

181

182 **Inside phagolysosomes individual LF82 were not homogenously responding to** 183 **stresses.**

184 Imaging revealed great heterogeneity in the number of LF82 bacteria within individual
185 macrophages. At 18 h or 24 h P.I., many macrophages presented fewer than 5 bacteria,
186 which was comparable to the amount observed at 1 h P.I. (Figure 2A); however, a
187 number of macrophages also presented foci containing up to 50 bacteria (Figure 2B).
188 These observations led us to consider that LF82 were not homogeneously stressed by
189 macrophages. We used GFP fusion with selected stress response promoters to monitor
190 variability of these responses among bacteria and among macrophages (Figure 2B). For
191 all stress responses, heterogeneity in GFP fluorescence was far larger than for LB
192 cultures (Figure 2 F - G). At 24 h P.I., we found that approximately 30% of the bacteria
193 had poorly respond to oxidative or acid responses (Figure 2E and 2F). Owing the high
194 stability of the GFP protein that we used in this assay, it is unlikely that this
195 heterogeneity resulted from short pulses of induction separated by long repression
196 periods. Such a sizeable phenotypic heterogeneity was moreover observed for bacteria
197 contained in a single macrophage as well as similar Lamp 1 positive vacuolar
198 environments (Figure 2C). We therefore questioned whether heterogeneity in stress
199 response might reflect the coexistence of multiple cell cycle regulation phenotypes.

200

201 **Macrophages induce the formation of non-growing LF82**

202 We assayed heterogeneity in LF82 cell cycle within macrophages by using two
203 complementary fluorescence assays. First, Fluorescent Dilution (FD) highlights bacteria
204 that have not divided since the time of infection (Figure 3A and Supplementary Figure
205 S4A-C).

206 FD shows that at 24 h P.I. LF82 underwent up to 6 divisions, which is still below the
207 maximum dilution detectable by the assay in our conditions (8 generations in LB,
208 Supplementary Figure S4B). In good agreement with the CFU measurement FD shown
209 that only 20% of the population has performed more than 1 division at 6 h P.I. From
210 these observations, we can estimate that the highest generation rate of LF82 within
211 macrophages is ≈ 0.5 doubling /h between 6 and 20 h P.I.. Interestingly, FD also revealed
212 that approximately 4% of the population did not divide or divided fewer than 2 times in
213 24 h P.I. (Figure 3A and Supplementary Figure S4B). By contrast among the small
214 amount of K12 bacteria that survived for 24 h in the macrophage, 60% of K12 bacteria
215 underwent fewer than 2 divisions and less than 10% underwent 5 divisions
216 (Supplementary Figure S3D). Second, we used TIMER to refine these observations; it
217 provides an instantaneous evaluation of the generation time during the infection
218 kinetics (Figure 3B and S4A and S4B). Timer indicated that 18 h post-infection, 18% of
219 the LF82 population was not actively dividing, supporting the existence of a non-
220 growing or slow-growing subpopulation. Since they require dilution of fluorescent
221 proteins both Timer and FD are poorly informative about the first hours of the infection.
222 Therefore, we used a GFP fusion with the septal ring protein FtsZ to monitor division in
223 the individual bacterium (Figure 3C). In LB, exponentially growing LF82 frequently
224 presented the FtsZ ring (70% of the population), but stationary phase LF82 rarely
225 presented the FtsZ ring (<2% of the population, Figure 3D). Following infection of
226 macrophages with the stationary phase culture of LF82 *ftsZ-gfp*, we observed that 5%
227 (+/-2) and 40% (+/- 12) of the population, respectively, presented a FtsZ ring at 1 h and
228 24 h P.I. (Figure 3C and 3D). Following infection with exponentially growing LF82 we
229 observed a sudden reduction in the number of LF82 presenting a FtsZ ring at 1 h and 4h
230 P.I. (Figure 3D). The three reporters (FD, Timer and FtsZ) provided complementary
231 indications: i) within macrophages, LF82 strongly slow down their cell cycle for several
232 hours; ii) starting at 6 h P.I. LF82 multiply; in this phase the generation time may vary
233 among bacteria but can be as short as 2h; iii) a part of the population, completely halted
234 their cell cycle and become non-grower. The difference between the number of non-
235 growing LF82 revealed by Timer and FD shows that non-growing LF82 are formed late
236 in the infection kinetics and not only upon phagocytosis.

237

238 **Macrophages induce the formation of antibiotic-tolerant LF82.**

239 Non-growing Salmonella phenotypes have been observed inside macrophages and
240 during mouse infection (Helaine *et al.*, 2014; Claudi *et al.*, 2014). Being tolerant to
241 subsequent antibiotic challenge they were recognized as persisters. We inquired
242 whether also for LF82 the non-growing component of the population had enhanced
243 antibiotic tolerance. In exponentially growing liquid cultures, approximately 1/10000
244 LF82 tolerated a 3 h ciprofloxacin challenge, and can therefore be considered persisters.
245 Following a brief passage through the macrophage, the frequency of LF82 bacteria
246 tolerant to ciprofloxacin increased to 0.5 % (nearly 50 fold compared to exponentially
247 growing LF82). Interestingly the number of tolerant LF82 increased to 5% (500 fold
248 compared exponentially growing LF82) after 24 h in the macrophage (Figure 4A). This
249 near to 10-fold increase at 24 h compared with 1 h indicates that, like non-growers,
250 tolerant phenotypes are not exclusively formed upon infection, but also as bacteria
251 multiply inside the macrophage. In this respect, the behavior of LF82 differs significantly
252 from *S. typhimurium*, which forms a large number of persisters upon macrophage entry ,
253 but this number remains stable during the infection (Helaine *et al.*, 2014). To test if non-
254 growing LF82 revealed by the FD assay indeed corresponded to the antibiotic-tolerant
255 population, we used the macrophage-permeable antibiotic ofloxacin. We added
256 ofloxacin (10x MIC) for 4 h after 20 h of intracellular growth, and we observed
257 significant increases in the proportion of green LF82 (non-growing) inside macrophages
258 (Figure 4B). These observations suggest that the sub-population of non-growing
259 bacteria largely overlaps with that of persisters, where protection from antibiotics may
260 also confer enhanced tolerance to intracellular stresses.

261

262 **Tolerance to antibiotics is enhanced for LF82 compared with commensal *E. coli*.**

263 We compared the number of LF82 and a commensal K12 laboratory strain with
264 tolerance to ciprofloxacin following brief (1 h) or long (24 h) passages in macrophages.
265 After a brief passage in macrophages, the proportion of LF82 that were tolerant to
266 ciprofloxacin was significantly higher for LF82 than K12 (Figure 4C). Interestingly, even
267 if the absolute number of ciprofloxacin-tolerant K12 was largely reduced compared with
268 LF82, their proportions among bacteria that survived 24 h inside macrophages were
269 comparable (Figure 4C). These findings demonstrate that the number of antibiotic-
270 tolerant bacteria formed in response to macrophage attack is reinforced for LF82
271 compared with a commensal strain.

272

273 **Tolerance to antibiotics is a transient state.**

274 We next evaluated whether the antibiotic tolerance was a stable or transient phenotype.
275 We used the macrophage lysis procedure to recover LF82 with induced persistence for 1
276 h in the macrophage; then, we either challenged them immediately with ciprofloxacin or
277 allowed them to recover in LB for 1 h or 2 h before antibiotic challenge. When bacteria
278 were cultured for 1 hour in LB, the frequency of tolerant bacteria was decreased in
279 comparison to bacteria that were immediately treated with the antibiotic; however, this
280 number was still higher than that of bacteria that had not infected macrophages. Two
281 hours in LB was sufficient to cause a comparable frequency of ciprofloxacin-tolerant
282 LF82 to that of bacteria that had not encountered macrophages (Figure 4D). These
283 observations show that when the environment is no longer stressful, antibiotic-tolerant,
284 non-growing LF82 rapidly switch back to a replicative mode.

285

286

287 **Characterization of non-growing LF82.**

288 Both FD and TIMER revealed slightly more non growing LF82 (4% and 18%
289 respectively, figure 3A) than antibiotic-tolerant LF82 after macrophage lysis (0.5% at 1
290 h P.I. or 5% at 24 h P.I. , Figure 4A). This finding raised the possibility that persisters
291 only form a portion of the non-growing population. To quantify this proportion, we
292 infected macrophages with TIMER-tagged LF82, lysed the macrophages and allowed
293 bacterial growth on a LB-agarose pad under the microscope at 37°C. Seventy percent of
294 the LF82 recovered quickly from the challenge and formed microcolonies, but
295 approximately 30% of them never divided (Figure 4E). These non-cultivable LF82
296 presented either non-growing and growing TIMER fluorescence (Figure 4F). The
297 presence of non-cultivable LF82 among the bacteria with non-growing TIMER
298 fluorescence explains the difference between fluorescence and antibiotics assays.

299

300 **SOS and stringent responses influence antibiotic tolerance.**

301 Among mutants that affected LF82 survival (Figure 1C), only the *recA*, *relA spot* and *dksA*
302 deletions negatively impacted the number of LF82 that were tolerant to a 3-h
303 ciprofloxacin treatment (Figure 5A). The impact of the *recA* deletion might be
304 misinterpreted because ciprofloxacin alters DNA and limits resuscitation of *recA*

305 persisters. Therefore, we repeated the tolerance assay with cefotaxime for the following
306 SOS mutants: *recA* (impaired for DNA lesion repair and SOS induction), *lexAind-* (unable
307 to induce SOS) and *sulA* (unable to block cell division). When they were tested *in vitro*,
308 SOS mutants did not present defect for cefotaxime tolerance (Supplementary Figure
309 S3B). However, these mutants exhibited decreased tolerance when persisters were
310 induced by a pretreatment with subinhibitory concentrations of ciprofloxacin
311 (Supplementary Figure S3C). This finding is in good agreement with previous reports
312 (Dörr *et al.*, 2009), it confirms that SOS induction favors the production of persisters.
313 We analyzed cefotaxime tolerance of these SOS mutants following 1 h and 20 h passages
314 within macrophages (Figure 5B and 5C). We observed for *recA* and *sulA* mutants a
315 significant reduction of the proportion of cells that were tolerant to cefotaxime
316 treatment after a 20 h passage in the macrophage (Figure 5C) but no immediate effect
317 for the 1 h time point (Figure 5B). The *lexAind-* mutant did not change the number of
318 tolerant LF82 in these conditions. We also analyzed the *dksA* mutant in these assays;
319 surprisingly, it behaved differently than the *recA* and *sulA* mutants: we observed a
320 significant reduction of the proportion of cefotaxime tolerant LF82 following a 1 h
321 passage within macrophages (Figure 5B) but not when the bacteria were grown for 20 h
322 in macrophages (Figure 5C). To test an eventual epistatic relation between SOS and
323 stringent response we combined *recA* and *dksA* deletions. They had an additive impact
324 on the ability of LF82 to become tolerant to cefotaxime after a brief infection (Figure 5B)
325 and a 20-hour infection (Figure 5C). Our observations suggest that production of
326 persister/tolerant LF82 is under the control of the stringent response in the first hours
327 of infection and controlled by genotoxic stress, the SOS response and DNA lesion
328 processing later in the infection. When one of these two responses is deficient the
329 production of persister /tolerant LF82 requires the other.

330

331 **The role of SOS response and stringent response for the control of LF82 cell cycle** 332 **in the macrophages.**

333 Knowing that SOS and stringent responses influence the production of antibiotic
334 tolerant LF82 after a passage within macrophage we examined whether SOS and
335 stringent responses also contributed to LF82 cell cycle control , i.e. production of non-
336 growing, replicative or dead LF82. We used the FD assay to measure the number of non-
337 growing LF82 in *the relA-spoT* and *recA* mutants. FD revealed that the non-grower

338 number was dramatically reduced in the *relA-spoT* mutant (<1%) (Figure 5D). This
339 suggests that in the absence of stringent response LF82 cannot immediately curb its cell
340 cycle upon phagocytosis. By contrast the number of non-growers remained unchanged
341 in the *recA* mutant (Figure 5E). This is in agreement with the absence of effect of the
342 *recA* deletion on the production of cefotaxime tolerant LF82 early in the infections.
343 TIMER revealed that at 20 h P.I. the proportion of slow, mid and fast growing LF82 was
344 affected by the alteration of *recA*, *lexAind-*, *sulA* and *dksA*. The *recA* and *dksA* deletions
345 reduced the number of non-growing LF82; by contrast, the *lexAind-* and *sulA* mutations
346 only increased the number of fast growing LF82 in the population (Figure 5F). Finally,
347 the live and dead assay showed a strong increase in lethality of the *recA*, *sulA*, *lexAind-*
348 *,relA spoT* and *dksA* mutants at both time points (Figure 5G) suggesting that in the
349 macrophage environment a failing cell cycle control will almost certainly lead to LF82
350 death. Altogether our results shown that stringent response is the main controller of the
351 early intracellular survival of LF82; it limits LF82 growth and induces the formation of
352 non-growers and among them persisters. Later on when replication is resumed SOS
353 response grows in importance. DNA lesions that have been accumulated in the lag phase
354 must be repaired to allow replication and formation of new non-growers and new
355 persisters.

356

357 **Kinetics of macrophage infection**

358 LF82 tolerates macrophage induced stresses, thus it survives and multiplies in the
359 phagolysosome. The population expansion is accompanied by a rise in the number of
360 bacteria that do not grow and tolerate an antibiotic challenge (called henceforth
361 persisters). The change in time, during macrophage infection, of LF82 population size
362 and fraction of persisters are relevant to future fundamental studies, but also to devising
363 therapeutic strategies involving AIEC or other intracellular pathogens. In order to
364 explore the mechanistic bases of the infection kinetics, we have used a mathematical
365 model (Figure 6A) to fit the observed changes in CFUs and persister counts during 24
366 hours for LF82, K12 and the stringent response mutant LF82*dksA* (Figure 6B). The
367 model is based on the following biologically-informed hypotheses (illustrated in Figure
368 6A and detailed in the Supplementary text 1). i) Reproduction: the population of
369 replicating bacteria B has a constant net growth rate (birth minus death rate) δ_1 , which
370 is either 0 or negative during a lag phase of duration λ , and $\beta > 0$ otherwise. ii) A stress-

371 induced death rate, $\delta_2(S)$ that increases with stress (S). We assume that stress S , possibly
372 due to lesions (DNA lesions, membranes alterations, oxidative damages among others)
373 that accumulate over time or due to a macrophage response to the infection, builds up in
374 time proportionally to the total number of bacteria in the population. iii) Switch to
375 persistence: bacteria have a constant probability k_p of generating non-growing, stress-
376 tolerant phenotypes P . The dynamics of a population of bacteria can be described by a
377 set of three ordinary differential equations for the number B of non-persister bacteria,
378 the number P of persisters, and the stress variable S (Methods). The number of dead
379 bacteria D can be derived from these under the assumption that dead LF82 decay
380 exponentially with rate 0.56 (computed from the assay in Supplementary Figure 2C).
381 The model has a total of 12 parameters for the three strains, which are fitted to data as
382 explained in Methods and SI. Although LF82 displays a considerable overshoot in
383 population size (as also observed in (Glasser *et al*, 2001)), the dynamics can be
384 reproduced by choosing the same β for every strain. We estimated such net growth rate
385 to $0.15 \pm 0.003 \text{ h}^{-1}$, corresponding to 0.21 divisions per hour (Figure 6B), consistent with
386 independent cell-level measures by FD (Supplementary Figure 4). The most notable
387 quantitative difference between strains is that K12 displayed a lag phase of more than
388 13 hours, twice as long as LF82 and LF82*dksA*. A consequence of this difference is that
389 when K12 bacteria start actively duplicating, stress has already built up. Together with
390 K12's enhanced sensitivity to stress, this curbs the population expansion, resulting in a
391 lower overall growth within macrophages. In the LF82*dksA* mutant, growth is instead
392 impaired by increased initial mortality (whose rate δ_1 has been estimated by PI
393 measures, Supplementary Figure S2C), presumably related to stringent response failure.
394 With respect to the other strains, moreover, LF82 is advantaged at later times – when
395 the SOS response becomes important – thanks to reduced stress-induced death rate.
396 Rate of persistence production for LF82 and LF82 *dksA* (0.08 and 0.002 h^{-1} , respectively)
397 is estimated to be higher than for K12 (0.001 h^{-1}), supporting the notion that AIEC
398 strains within macrophages turn to persisters at an enhanced rate, but less so if their
399 stringent response is impaired. The model allows testing changes in infection dynamics
400 for 'virtual mutants' LF82*, obtained by varying k_p , λ and d_{\max} – the parameters that
401 quantitatively differ between LF82 and *E. coli* K12 (Figure 6C). The total population
402 overshoot is enhanced when lag phase is shorter and the effect of stress less acute, but
403 damped when persisters production is more frequent. Interestingly, the phenotypes of

404 the single stress response mutants (acid, oxidative, lack of Mg^{2+}), i.e. reduced CFU at 24 h
405 without perturbation of the persister proportion in the population (Figure 1C and 3A)
406 were nicely reproduced by a change in the single d_{max} parameter. This suggests that the
407 model can be used to plan future works on the effect of mutants or drugs on macrophage
408 colonization by LF82.

409

410

411 **Discussion**

412 We analyzed the growth and survival strategies used by LF82 to colonize the THP1
413 macrophage cell line. Our analysis revealed that intracellular LF82 were constantly
414 under stress while colonizing macrophages. The consequences of these stresses were
415 important: increase in the death rate of LF82, slow multiplication of replicating LF82
416 and formation of a large number of non-growing LF82. LF82 adapts to this environment
417 thanks to successive phenotypic switches that require the two main stress responses:
418 the SOS response and the stringent response (Figure 7).

419

420 **Macrophages place LF82 under lethal stress.**

421 Using fluorescent reporters, we measured that half of the LF82 population present at 24
422 h P.I. had given rise to 6 or more generations. Under normal condition, this should
423 produce a 30 to 60-fold increase in the population size at 20 h compared with the 1 h
424 time point PI. However, we only observed a 3 to 6-fold increase in viable bacteria at 20-
425 24 h compared with 1 h. We demonstrated that this modest colonization of
426 macrophages by LF82 is explained by a big death rate (Figure 1A) and switch from
427 replicative to non-growing cell cycle (Figure 3). At the single-macrophage and single-
428 bacterium level, FD and TIMER fluorescent reporters revealed non-growing LF82. We
429 observed macrophages containing few (less than 4) LF82 with red fluorescent dilution
430 staining. These bacteria had therefore divided several times (>4) before observation and
431 thus should be accompanied by their siblings (>16). This observation is in good
432 agreement with our Live and Dead assay indicating that LF82 progeny has a significant
433 chance to be killed and destroyed by the macrophage. By contrast, some macrophages
434 contained growing LF82 and ultimately acquired more than 50 bacteria in one or
435 several compartments. The live and dead assay confirmed that LF82 was frequently
436 killed by macrophages. Because alterations of bacterial stress responses significantly

437 reduced the bacterial yield, we propose that LF82 death is the consequence of oxidative,
438 acid, genotoxic and proteic stresses imposed by the macrophage. We compounded these
439 experimental observations in a mathematical model describing the dynamics of
440 bacterial infection within macrophages. A first phase of stalled growth, a likely
441 combined effect of a prolonged lag phase and of compensation between death and
442 division, is followed by an exponential increase in bacterial concentration. This second
443 phase might correlate with a transient increased permissiveness of phagolysosomes or
444 more likely the adaptation of LF82 to growth in this stressful environment. This
445 expansion is successively curbed by the building-up of stressors. Many persisters are
446 formed in the first phase. However, in the second phase a phenotypic switch to non-
447 growing LF82 will eventually result in a sizeable increase of the persister population.
448 We thus understand the survival of LF82 as a consequence of its ability to adapt to harsh
449 phagolysosome environment both at the entry of the macrophage, by induction of stress
450 responses and particularly the stringent response, and during exponential expansion by
451 SOS response. LF82 advantage over commensal K12 would reside in its ability to exit
452 from the lag phase to perform a few rounds of replication/division before stress
453 becomes too strong (Figure 6). Strategically, early onset of growth is compensated by
454 production of persistent bacteria, which endows the pathogenic strain with long-term
455 survival in spite of rapid exploitation of the macrophage environment. We have not yet
456 identified LF82 specific regulons, genes or mutations that allow this transition to take
457 place.

458

459 **Replicative LF82.**

460 Fluorescent dilution revealed that after the exit of lag phase LF82 replicated moderately
461 within macrophages, with generation time longer than 2 h. *In vitro*, this would be
462 comparable with generation times observed in minimal medium with poor carbon
463 sources such as acetate. Our observations revealed that within macrophages, 40% of the
464 LF82 population presented an FtsZ ring, which is significantly above the number
465 expected from a mixed population of *E. coli* growing with a 2h generation time (28% of
466 cells with FtsZ ring (den Blaauwen *et al*, 2001)) and non-growing cells. Interestingly, in
467 spite of SulA induction, we did not observe filamentation of LF82 within macrophage.
468 These finding demonstrates that some of the cell cycle rules that were established under
469 defined *in vitro* conditions do not apply to intracellular growth conditions, opening

470 avenues for future investigations of bacterial cell cycle regulation in the context of host
471 infection or the microbiota.

472

473 **Non-replicative LF82.**

474 FD and Timer revealed that a significant number of intracellular LF82 were not growing.
475 FD revealed that approximately 4% of the phagocytosed LF82 immediately halted their
476 cell cycle. TIMER revealed that at 20 h P.I., approximately 20% of the LF82 population
477 was not growing. We also demonstrated that once the macrophages were lysed, a large
478 portion of the LF82 population (from 0.3 to 10%) was tolerant to several hours of
479 antibiotic challenge, and the proportion of non-growers in the population increased in
480 macrophages in the presence of antibiotics. Altogether, these observations suggest that
481 the phagolysosome environment induces frequent cell cycle arrests among the
482 population and that a part of this arrested population is tolerant or persists to
483 antibiotics. Such a phenomenon has been previously described during *S. typhimurium*
484 infection of macrophages (Helaine *et al.*, 2014) or mice (Helaine *et al.*, 2014; Claudi *et al.*,
485 2014) and is reminiscent of VBNR mycobacteria (Manina *et al.*, 2015). Interestingly, we
486 observed an increase in the proportion of macrophage-induced antibiotic-tolerant LF82
487 at later time points, suggesting adaptive responses to the intracellular
488 microenvironment.

489

490 **Stress responses are important for LF82 survival within macrophages.**

491 As expected for bacteria residing in a toxic environment, stress responses are important
492 for LF82 survival within macrophages. Acidic, oxidative, genotoxic, and envelope
493 alterations, lack of Mg²⁺ and lack of nutrient stress responses significantly decreased
494 the fitness of LF82 (50 to 10% of WT). In a few cases, we demonstrated an additive
495 effect of simultaneously altering two pathways. However, LF82 demonstrated
496 surprisingly good tolerance to these alterations compared with the *in vitro* findings for
497 individual stresses. For example, *recA* deletion mutant was extremely sensitive (<1%
498 survival) to prolonged treatment with genotoxic drugs (Supplementary Figure S3A); by
499 comparison, in macrophages, despite clear SOS induction, the viability of the *recA*
500 mutant was only reduced by half compared with WT. Set aside the possibility that
501 stress-less niches exist due a possible heterogeneity in the macrophage population, the

502 fitness decline of LF82 stress mutants may be limited by a combination of slow growth,
503 formation of non-growers and/or yet uncharacterized adaptation pathways.

504

505 **SOS and stringent responses successively control LF82 fate.**

506 We investigated the trigger that could allow some LF82 to halt their cell cycle inside
507 macrophages. It appeared to be unrelated to the ability to sense acidic or oxidative
508 stress (Figure 5A). At an early time point (1 h P.I.), stringent response mutants
509 significantly altered the survival and production of antibiotic-tolerant LF82 (Figure 1
510 and Figure 5A). This finding suggests that abrupt nutrient starvation is one of the first
511 signals received by LF82 upon phagocytosis. The early stringent response should result
512 in a slowdown of transcription, translation and DNA replication, and therefore, it might
513 provoke the formation of non-growers and a lag phase that last for 7 h (Figure 6). We
514 assessed whether the stringent response impaired the declines in viability in this first
515 period (Figure 5), and we observed a decrease in the number of bacteria with undiluted
516 GFP using the FD assay (Figure 5D), as well as a reduction in antibiotic-tolerant LF82
517 induction (Figure 5B). This suggests that the slowing down induced by the stringent
518 response confers a temporary protection than can be extended to antibiotic tolerance
519 when bacteria become persister. Accordingly the impact of stringent response alteration
520 was less apparent after the lag phase when replication is re-established in a portion of
521 the population of LF82 (Figure 5). SOS induction was moderate at 1 h but important at 6
522 h and 24 h P.I.; this is in good agreement with the lack of an effect of *recA* deletion on the
523 accumulation of LF82 with undiluted FD GFP (Figure 5D) and the lack of an influence of
524 SOS mutants on the number of LF82 that were tolerant to cefotaxim at 1 h after infection
525 (Figure 5B). DNA lesions could, however, form during this period, but they were mostly
526 observed when DNA replication restarted after 6 h. In this second phase of infection, SOS
527 induction in replicative bacteria might play several roles: i) sustaining DNA repair and
528 therefore DNA replication, cell division and increases in population size; ii) decelerating
529 the division progression, this is the role of Sula, and thus contributing to the formation
530 of new non-growers (Figure 5C and 5D and Figure 7); iii) intervening for resuscitation of
531 non-growers presenting DNA lesions, both within macrophages and after macrophage
532 lysis.

533

534 **Macrophages as a niche for LF82 survival**

535 The purpose of macrophage colonization by LF82 in Crohn's disease patients is not yet
536 understood. *In vitro*, LF82 colonization did not provoke extensive death of macrophages,
537 which are thus unlikely to serve as a transient replicative niche for ileal infection.
538 Alternatively, we can imagine that dormant LF82 within macrophages can serve as a
539 long-term storage. In this environment, bacteria might be protected from competition
540 with other species of the microbiota and coincidentally from antibiotics. Upon
541 macrophage lysis or inactivation, dormant LF82 would be released and would start to
542 multiply under adequate conditions.

543

544 **Methods**

545 **Strains and plasmids**

546 Deletion mutants (Supplementary Table S1) were constructed using the recombineering
547 method as described in (Demarre *et al.*, 2017). Plasmids are described in Supplementary
548 Table S2.

549

550 **Infection and microscopy**

551 THP1 monocytes (5×10^5 cells/ml) differentiated into macrophages for 18 h in phorbol
552 12-myristate 13-acetate (PMA, 20 ng/ml) were infected and imaged as previously
553 described (Demarre *et al.*, 2017). Infections were performed using an MOI of 30
554 (measured by CFU), resulting in the observation of 3 LF82 bacteria per macrophage on
555 average at 1 h post-infection. Imaging was performed on an inverted Zeiss Axio Imager
556 with a spinning disk CSU W1 (Yokogawa).

557

558

559 **Antibiotic challenge and viable bacterial count using the gentamycin protection** 560 **assay**

561 To determine the number of intracellular bacteria after 20 min of infection, infected
562 macrophages were washed twice with PBS, and fresh cell culture medium containing 20
563 $\mu\text{g ml}^{-1}$ of gentamicin (Gm) was added for the indicated time (1 h to 30 h). Cell
564 monolayers were washed once with PBS, and 0.5 ml of 1% Triton X-100 in 1x PBS was
565 added to each well for 5 min to lyse eukaryotic cells (Bringer *et al.*, 2006). Samples were
566 mixed, diluted and plated on LB agar plates to determine the number of colony-forming
567 units (CFU) recovered from the lysed monolayers. For the antibiotic tolerance assays,

568 macrophage lysates were transferred to 5-ml tubes and centrifuged for 10 min at 4100
569 g. The pellet was either resuspended in 1x PBS (t0) and ciprofloxacin (1 µg/ml) for 1 h
570 and 3 h, or in LB and cefotaxim (100 µg/ml) for 1 h and 3 h. CFU were measured by
571 serial dilution. Tolerance was estimated for the 1-h and 3-h time points as a function of
572 the CFU at t0.

573

574 **Live and dead assay**

575 At the indicated time points, macrophages were lysed with vigorous resuspension in 1x
576 PBS 1% Triton. The cell lysate was pelleted at 300 g for 10 min to eliminate large cell
577 remnants. The supernatant was centrifuged at 4000 g for 10 min. The bacterial pellet
578 was suspended in 1x PBS and processed with the Live and Dead BacLight Viability kit
579 (Thermo Fisher). The bacteria were pelleted for 3 min at 5000 g, resuspended in 50 µl of
580 1x PBS and spread on a 1% agarose 1x PBS pad for immediate observation.

581

582 **Measurement of gene expression by RT-qPCR**

583 Total RNA was extracted with TRIzol reagent from 10⁶ macrophages, as described in the
584 *Molecular Cloning, a laboratory Manual* (Green and Sambrook, CSH Press). First-strand
585 CDNA synthesis was performed with the Maxima First Strand cDNA Synthesis Kit for RT-
586 qPCR (Thermo Fisher), and real-time qPCR was performed with SYBR Green Master Mix
587 (Bio-Rad) on a MyiQ real-time qPCR machine (Bio-Rad).

588

589 **Fluorescence quantification**

590 Custom-made FIJI macros were developed for the analyses of fluorescence. For the
591 Biosensors and FD, constitutive expression of mCherry from p-mCherry was used to
592 construct bacterial masks, which were subsequently used to measure GFP intensity. For
593 TIMER analyses, green fluorescence was used to construct the mask. Fluorescence
594 distributions were analyzed with the distribution fitting tool in MATLAB.

595

596 **Mathematical model for the infection kinetics**

597 A set of three ODEs recapitulates the main features of the observed growth within
598 macrophages, as explained in the main text and in the SI:

$$\begin{aligned}\frac{dB}{dt} &= [1 - I(t < \lambda)]\beta B - k_p B - I(t < \lambda)\delta_1 B - \delta_2(S)B \\ \frac{dP}{dt} &= k_p B \quad (1) \\ \frac{dS}{dt} &= B + P\end{aligned}$$

599 Here, $I(t < \lambda)$ is the indicator function, which is unitary during lag phase. At the
600 beginning of the infection, thus, the net growth rate $-\delta_1$ is either zero (K12 and LF82) or
601 negative (stringent response mutant LF82dskA). At later times, net growth rate β is
602 instead positive. The stress-induced death rate has been chosen to be a sigmoidal
603 function of the stress level:

$$604 \quad \delta_2(S) = \frac{d_{max}}{1 + e^{a(S - S_{1/2})}}$$

605 where the half-saturation stress value $S_{1/2}$ and the sensitivity parameter a are assumed
606 to be identical for all strains. Here stress is an effective variable quantifying the effect of
607 crowding on growth within macrophages, and could correspond both to density-
608 dependent reduction of bacterial growth rate (e.g. due to resource depletion), and to the
609 progressive buildup of macrophage-induced killing.

610

611 **Fit of the infection kinetics data**

612 Parameters providing the best fit of eqs. (1) to the times series of CFUs and persisters
613 have been obtained by a weighted least-square distance minimization using the python
614 differential evolution algorithm. We used a two-step approach to the fit which allowed us to
615 establish first a subset of 7 parameters (λ and k_p for each strain and β) that shape the lag
616 and exponential phases of growth. Subsequently, we fixed β and the λ s, and fitted the
617 remaining parameters. Details of the fitting procedure are found in the SI, and the
618 results of the fit in Table 1 of the SI.

619

620

621 **Acknowledgments**

622 We gratefully acknowledge Laurent Aussel, Dirk Bumann, Sophie Helaine, Jakob Moller
623 Jensen and Fabai Wu for providing the biosensors and fluorescent cell cycle reporters.
624 We thank Parul Singh and Xavier de Bolle for careful reading of the manuscript and
625 fruitful discussions. We are very grateful to the members of the CIRB imaging facility.
626 This work has received support from the program «Investissements d’Avenir » launched

627 by the French Government and implemented by ANR with the references ANR--10--
628 LABX--54 MEMOLIFE and ANR--11--IDEX--0001--02 PSL* Research University, from the
629 ANR with the reference ANR-18-CE35-0007 and the support of the association François
630 Aupetit (AFA).
631
632

633 Table S1

Name	genotype	description	reference
AIEC LF82			(Glasser <i>et al.</i> , 2001)
AIEC LF82 Δ bla	<i>ampC</i>		Gift from Nicolas Barnich
AIEC LF82 Δ htrA	<i>htrA</i>		(Bringer <i>et al.</i> , 2005)
AIEC LFGD1	AIEC LF82 Δ bla <i>relA::kan</i>		This work
AIEC LFGD4	AIEC LF82 Δ bla <i>ydeO::kan</i>		This work
AIEC LFGD6	AIEC LF82 Δ bla <i>lon::kan</i>		This work
AIEC LFGD9	AIEC LF82 Δ bla <i>recA::kan</i>		This work
AIEC LFGD11	AIEC LF82 LF82 Δ bla <i>HupA-mcherry-FRT-kan-FRT</i>		This work
AIEC LFGD13	AIEC LF82 Δ bla <i>pspA::kan</i>		This work
AIEC LFGD15	AIEC LF82 Δ bla <i>soxS::kan</i>		This work
AIEC LFGD27	AIEC LF82 Δ bla <i>phoP::kan</i>		This work
AIEC LFGD30	AIEC LF82 Δ bla <i>evgA evgS::kan</i>		This work
AIEC LFGD40	AIEC LF82 Δ bla <i>evgAS-FRT phoP::kan</i>		This work
AIEC LFGD41	AIEC LF82 Δ bla <i>evgA evgS-FRT ydeO::kan</i>		This work
AIEC LFGD56	AIEC LF82 Δ bla <i>relA-FRT</i>		This work
AIEC LFGD57	AIEC LF82 Δ bla <i>relA-FRT spoT::kan</i>		This work
AIEC LFGD69	AIEC LF82 Δ bla <i>lexA ind-::kan</i>	Mutation X-> Y in <i>lexA</i> constructed by recombineering	This work
AIEC LFGD79	AIEC LF82 Δ bla <i>dksA::kan</i>		This work

AIEC LFER1	AIEC LF82 <i>Δbla lexAind-FRT dksA::kan</i>		This work
AIEC LFER2	AIEC LF82 <i>Δbla dksA-FRT recA::kan</i>		This work
AIEC LFGD86	AIEC LF82 <i>Δbla sula::kan</i>		This work
AIEC LFGD83	AIEC LF82 <i>Δbla ppk-ppX::kan</i>		This work
AIEC LF82 Δ rpoS	<i>rpoS::kan</i>		Gift from Jakob Moller Jensen (Simonsen <i>et al.</i> , 2011)

634

635

636 Table S2

name	description	Antibiotic resistance	reference
pKOBEGA		ampR specR	(Derbise <i>et al.</i> , 2003)
pAD37	Matrix vector for recombineering	kanR	(David <i>et al.</i> , 2014)
pFWZ5	Para-fts-sfGFP-T::aph	kanR	Gift from Fabai Wu (Wu <i>et al.</i> , 2015)
pFCcGi	pFP25 <i>PrpsM-mCherry</i> , ParaBAD-GFP	ampR	Gift from Sophie Helaine (Helaine <i>et al.</i> , 2014)
pPrpsm-mcherry	pGBM2- <i>PrpsM-mCherry</i>	specR	This work
pSC101-timer bac			Gift from Dirk Bumann (Claudi <i>et al.</i> , 2014)
pom1-GFP	pGBM2-Pro3-GFP		(Espéli <i>et al.</i> , 2001)

pLA42	pFPV25 PkatG-gfpmut3	ampR	Gift from Laurent Aussel (Viala <i>et al.</i> , 2011; Hébrard <i>et al.</i> , 2009)
pP1485	pFPV25 <i>Pasr-gfp</i>	ampR	Gift from Laurent Aussel (Viala <i>et al.</i> , 2011; Hébrard <i>et al.</i> , 2009)
pmgtC	pFPV25 <i>PmgtC-gfp</i>	ampR	Gift from Laurent Aussel (Viala <i>et al.</i> , 2011; Hébrard <i>et al.</i> , 2009)
pSulA-GFP	pZA31MCS-delta Xho <i>PsulA-GFP</i>		(Esnault <i>et al.</i> , 2007)

637

638

639 **References**

- 640 Amato SM & Brynildsen MP (2015) Persister Heterogeneity Arising from a Single
641 Metabolic Stress. *Curr. Biol. CB* **25**: 2090–2098
- 642 Amato SM, Fazen CH, Henry TC, Mok WWK, Orman MA, Sandvik EL, Volzing KG &
643 Brynildsen MP (2014) The role of metabolism in bacterial persistence. *Front.*
644 *Microbiol.* **5**: 70
- 645 Balaban NQ, Merrin J, Chait R, Kowalik L & Leibler S (2004) Bacterial persistence as a
646 phenotypic switch. *Science* **305**: 1622–1625
- 647 Barnich N, Bringer M-A, Claret L & Darfeuille-Michaud A (2004) Involvement of
648 lipoprotein NlpI in the virulence of adherent invasive Escherichia coli strain LF82
649 isolated from a patient with Crohn's disease. *Infect. Immun.* **72**: 2484–2493
- 650 Bernier SP, Lebeaux D, DeFrancesco AS, Valomon A, Soubigou G, Coppée J-Y, Ghigo J-M &
651 Beloin C (2013) Starvation, together with the SOS response, mediates high
652 biofilm-specific tolerance to the fluoroquinolone ofloxacin. *PLoS Genet.* **9**:
653 e1003144
- 654 Bigger J (1944) TREATMENT OF STAPHYLOCOCCAL INFECTIONS WITH PENICILLIN BY
655 INTERMITTENT STERILISATION. *The Lancet* **244**: 497–500
- 656 den Blaauwen T, Lindqvist A, Löwe J & Nanninga N (2001) Distribution of the
657 Escherichia coli structural maintenance of chromosomes (SMC)-like protein
658 MukB in the cell. *Mol. Microbiol.* **42**: 1179–1188
- 659 Bringer M-A, Barnich N, Glasser A-L, Bardot O & Darfeuille-Michaud A (2005) HtrA
660 stress protein is involved in intramacrophagic replication of adherent and
661 invasive Escherichia coli strain LF82 isolated from a patient with Crohn's disease.
662 *Infect. Immun.* **73**: 712–721
- 663 Bringer M-A, Billard E, Glasser A-L, Colombel J-F & Darfeuille-Michaud A (2012)
664 Replication of Crohn's disease-associated AIEC within macrophages is dependent
665 on TNF- α secretion. *Lab. Investig. J. Tech. Methods Pathol.* **92**: 411–419
- 666 Bringer M-A, Glasser A-L, Tung C-H, Méresse S & Darfeuille-Michaud A (2006) The
667 Crohn's disease-associated adherent-invasive Escherichia coli strain LF82
668 replicates in mature phagolysosomes within J774 macrophages. *Cell. Microbiol.* **8**:
669 471–484
- 670 Bringer M-A, Rolhion N, Glasser A-L & Darfeuille-Michaud A (2007) The oxidoreductase
671 DsbA plays a key role in the ability of the Crohn's disease-associated adherent-
672 invasive Escherichia coli strain LF82 to resist macrophage killing. *J. Bacteriol.*
673 **189**: 4860–4871
- 674 Cieza RJ, Hu J, Ross BN, Sbrana E & Torres AG (2015) The IbeA invasin of adherent-
675 invasive Escherichia coli mediates interaction with intestinal epithelia and
676 macrophages. *Infect. Immun.* **83**: 1904–1918

- 677 Claudi B, Spröte P, Chirkova A, Personnic N, Zankl J, Schürmann N, Schmidt A & Bumann
678 D (2014) Phenotypic variation of Salmonella in host tissues delays eradication by
679 antimicrobial chemotherapy. *Cell* **158**: 722–733
- 680 David A, Demarre G, Muresan L, Paly E, Barre F-X & Possoz C (2014) The two Cis-acting
681 sites, parS1 and oriC1, contribute to the longitudinal organisation of Vibrio
682 cholerae chromosome I. *PLoS Genet.* **10**: e1004448
- 683 Demarre G, Prudent V & Espéli O (2017) Imaging the Cell Cycle of Pathogen E. coli
684 During Growth in Macrophage. *Methods Mol. Biol. Clifton NJ* **1624**: 227–236
- 685 Derbise A, Lesic B, Dacheux D, Ghigo JM & Carniel E (2003) A rapid and simple method
686 for inactivating chromosomal genes in Yersinia. *FEMS Immunol. Med. Microbiol.*
687 **38**: 113–116
- 688 Dörr T, Lewis K & Vulić M (2009) SOS response induces persistence to fluoroquinolones
689 in Escherichia coli. *PLoS Genet.* **5**: e1000760
- 690 Elhenawy W, Oberc A & Coombes BK (2018) A polymicrobial view of disease potential in
691 Crohn's-associated adherent-invasive E. coli. *Gut Microbes* **9**: 166–174
- 692 Esnault E, Valens M, Espéli O & Boccard F (2007) Chromosome structuring limits
693 genome plasticity in Escherichia coli. *PLoS Genet.* **3**: e226
- 694 Espéli O, Moulin L & Boccard F (2001) Transcription attenuation associated with
695 bacterial repetitive extragenic BIME elements. *J. Mol. Biol.* **314**: 375–386
- 696 Glasser AL, Boudeau J, Barnich N, Perruchot MH, Colombel JF & Darfeuille-Michaud A
697 (2001) Adherent invasive Escherichia coli strains from patients with Crohn's
698 disease survive and replicate within macrophages without inducing host cell
699 death. *Infect. Immun.* **69**: 5529–5537
- 700 Haeusser DP & Levin PA (2008) The great divide: coordinating cell cycle events during
701 bacterial growth and division. *Curr. Opin. Microbiol.* **11**: 94–99
- 702 Hajduk IV, Rodrigues CDA & Harry EJ (2016) Connecting the dots of the bacterial cell
703 cycle: Coordinating chromosome replication and segregation with cell division.
704 *Semin. Cell Dev. Biol.* **53**: 2–9
- 705 Harms A, Fino C, Sørensen MA, Semsey S & Gerdes K (2017) Prophages and Growth
706 Dynamics Confound Experimental Results with Antibiotic-Tolerant Persister
707 Cells. *mBio* **8**:
- 708 Hébrard M, Viala JPM, Méresse S, Barras F & Aussel L (2009) Redundant hydrogen
709 peroxide scavengers contribute to Salmonella virulence and oxidative stress
710 resistance. *J. Bacteriol.* **191**: 4605–4614
- 711 Helaine S, Cheverton AM, Watson KG, Faure LM, Matthews SA & Holden DW (2014)
712 Internalization of Salmonella by macrophages induces formation of
713 nonreplicating persisters. *Science* **343**: 204–208

- 714 Jonas K (2014) To divide or not to divide: control of the bacterial cell cycle by
715 environmental cues. *Curr. Opin. Microbiol.* **18**: 54–60
- 716 Kim J-S & Wood TK (2017) Tolerant, Growing Cells from Nutrient Shifts Are Not
717 Persister Cells. *mBio* **8**:
- 718 Kreuzer KN (2013) DNA damage responses in prokaryotes: regulating gene expression,
719 modulating growth patterns, and manipulating replication forks. *Cold Spring*
720 *Harb. Perspect. Biol.* **5**: a012674
- 721 Lapaquette P, Bringer M-A & Darfeuille-Michaud A (2012) Defects in autophagy favour
722 adherent-invasive Escherichia coli persistence within macrophages leading to
723 increased pro-inflammatory response. *Cell. Microbiol.* **14**: 791–807
- 724 Lewis K (2010) Persister cells. *Annu. Rev. Microbiol.* **64**: 357–372
- 725 Manina G, Dhar N & McKinney JD (2015) Stress and host immunity amplify
726 Mycobacterium tuberculosis phenotypic heterogeneity and induce nongrowing
727 metabolically active forms. *Cell Host Microbe* **17**: 32–46
- 728 Margolin W & Bernander R (2004) How do prokaryotic cells cycle? *Curr. Biol. CB* **14**:
729 R768-770
- 730 Miquel S, Claret L, Bonnet R, Dorboz I, Barnich N & Darfeuille-Michaud A (2010) Role of
731 decreased levels of Fis histone-like protein in Crohn's disease-associated
732 adherent invasive Escherichia coli LF82 bacteria interacting with intestinal
733 epithelial cells. *J. Bacteriol.* **192**: 1832–1843
- 734 Mouton JM, Helaine S, Holden DW & Sampson SL (2016) Elucidating population-wide
735 mycobacterial replication dynamics at the single-cell level. *Microbiol. Read. Engl.*
736 **162**: 966–978
- 737 Radzikowski JL, Vedelaar S, Siegel D, Ortega AD, Schmidt A & Heinemann M (2016)
738 Bacterial persistence is an active σ S stress response to metabolic flux limitation.
739 *Mol. Syst. Biol.* **12**: 882
- 740 Rao NN & Kornberg A (1999) Inorganic polyphosphate regulates responses of
741 Escherichia coli to nutritional stringencies, environmental stresses and survival
742 in the stationary phase. *Prog. Mol. Subcell. Biol.* **23**: 183–195
- 743 Rycroft JA, Gollan B, Grabe GJ, Hall A, Cheverton AM, Larrouy-Maumus G, Hare SA &
744 Helaine S (2018) Activity of acetyltransferase toxins involved in
745 Salmonella persister formation during macrophage infection. *Nat. Commun.* **9**:
746 1993
- 747 Shan Y, Brown Gandt A, Rowe SE, Deisinger JP, Conlon BP & Lewis K (2017) ATP-
748 Dependent Persister Formation in Escherichia coli. *mBio* **8**:
- 749 Sharma UK & Chatterji D (2010) Transcriptional switching in Escherichia coli during
750 stress and starvation by modulation of sigma activity. *FEMS Microbiol. Rev.* **34**:
751 646–657

- 752 Simonsen KT, Nielsen G, Bjerrum JV, Kruse T, Kallipolitis BH & Møller-Jensen J (2011) A
753 role for the RNA chaperone Hfq in controlling adherent-invasive *Escherichia coli*
754 colonization and virulence. *PloS One* **6**: e16387
- 755 Verstraeten N, Knapen W, Fauvart M & Michiels J (2016) A Historical Perspective on
756 Bacterial Persistence. *Methods Mol. Biol. Clifton NJ* **1333**: 3–13
- 757 Viala JPM, Méresse S, Pocachard B, Guilhon A-A, Aussel L & Barras F (2011) Sensing and
758 adaptation to low pH mediated by inducible amino acid decarboxylases in
759 *Salmonella*. *PloS One* **6**: e22397
- 760 Wood TK, Knabel SJ & Kwan BW (2013) Bacterial persister cell formation and
761 dormancy. *Appl. Environ. Microbiol.* **79**: 7116–7121
- 762 Wu F, Van Rijn E, Van Schie BGC, Keymer JE & Dekker C (2015) Multi-color imaging of
763 the bacterial nucleoid and division proteins with blue, orange, and near-infrared
764 fluorescent proteins. *Front. Microbiol.* **6**: 607
- 765
- 766

767 **Legend of the figures**

768 **Figure 1.** A) Measure of viable and dead AIEC LF82 for 24 h post-infection of THP1
769 differentiated macrophages. Circles represent average CFU (blue) and Propidium iodide
770 (PI) positive bacteria (black) \pm Standard deviation (SD) (dotted lines). B) Analysis by
771 qRT-PCR of the induction of LF82 stress responses at 1 h, 6 h and 24 h P.I. of THP1
772 macrophages. Values represent the average of two experiments. C) Proportion of viable
773 bacteria at 24 h P.I. of THP1 macrophages in comparison to 1 h. LF82, K12 and LF82
774 deletion mutants were infected at a MOI of 30 which corresponds to 0 - 5 visible bacteria
775 per macrophage at time point 1h (Figure 2A). Values represent the average of 3 to 7
776 experiments \pm SD. Horizontal lines indicate viability decrease by 2, 5 and 10 fold
777 compared to WT LF82.

778
779 **Figure 2.** A) Imaging of THP1 macrophages infection by LF82-GFP at a MOI of 30.
780 Representative images at 1 h and 24 h. Scale bar is 5 μ m B) Imaging of LF82-mCherry
781 stress responses at the single cell level with biosensors. Imaging was performed at 24 h
782 P.I.. LF82-mCherry was transformed with plasmids containing either the *katG* promoter
783 fused to GFP (*PkatG*-GFP), the *mgtC* promoter (*PmgtC*-GFP), the *asr* promoter (*Pasr*-
784 GFP) or the *sulA* promoter (*PsulA*-GFP). C) Imaging of LF82-mCherry *Pasr*GFP and
785 Lamp1 phagolysosome marker E) Measure of the fluorescence intensity of individual
786 LF82-mCherry containing the *katG* promoter fused to GFP at 1 h and 24 h P.I. F) Measure
787 of the fluorescence intensity of individual LF82-mCherry containing the *asr* promoter
788 fused to GFP at 1 h and 24 h P.I. G) LF82 *PsulA*-GFP, LF82 *PkatG*GFP, LF82 *Pasr*-GFP in
789 LB respectively supplemented with MMC (5 μ M), with H₂O₂ (5 μ M) or switched to pH4.7
790 1h before imaging. Distribution of the fluorescence of LF82 *Pasr*-GFP after 24h post
791 infection in macrophage (from panel B) and after 1 hours of growth in LB buffered at
792 pH4.7. Fluorescence values were expressed as their log₂ratio with the average value of
793 the maximum decile (maximum expression). Distributions were compared with a Two-
794 sample Kolmogorov-Smirnov (KS) test.

795
796 **Figure 3.** A) Representative image of LF82 containing the fluorescent dilution plasmid
797 (pFC6Gi) at 1 h and 24 h post-infection. The frequency of replicative and non-growing
798 LF82 (undiluted GFP) is indicated (N =300). B) Representative image of LF82 containing
799 the TIMER plasmid (pBR-TIMER) at 18 h post-infection. The red arrows points toward

800 the reddest LF82. The frequency of replicative and non-growing LF82 is indicated (N
801 =300). C) Representative images of LF82-mCherry FtsZ-GFP at 1 h and 24 h post-
802 infection. Infections presented in panels A to C were performed with a stationary phase
803 culture of LF82 (O.D. 2). Scale bars are 5 μ m. D) Measure of the frequency of LF82
804 presenting a FtsZ ring in populations growing in LB or within macrophages (N =300).

805

806 **Figure 4.** A) Measure of the proportion of LF82 that were tolerant to ciprofloxacin (10x
807 MIC) at 1 h or 3 h. LF82 were cultivated up to OD 0.3 in LB medium (*in vitro*) or
808 harvested after 1 h or 24 h post infection within macrophages. The challenges exerted
809 on bacteria passaged through macrophages started immediately after macrophage lysis
810 (see experimental procedures). B) Proportion of non-growing LF82 (labeled using the
811 Fluorescent Dilution assay) observed within macrophages (24 h P.I.) following a 6 h
812 ofloxacin treatment. C) Ratio of ciprofloxacin-tolerant versus viable LF82 and K12
813 bacteria after macrophage infection. Values are averages of 5 experiments. Data were
814 analyzed using a Student's *t* test to determine differences with the proportion of
815 ciprofloxacin-tolerant LF82 at 1 h post-infection, **P* < 0.05. D) Measure of the
816 proportion of LF82 that were tolerant to ciprofloxacin at 1 h or 3 h with increasing times
817 after macrophage lysis. E) Imaging of the regrowth properties of individual LF82-TIMER
818 bacteria after macrophages lysis. Infections were performed for 20 h and then
819 macrophages were lysed, LF82 spread on to LB agarose pads and immediately imaged at
820 37°C. Timer red fluorescence was progressively lost as microcolonies formed. The lysis
821 procedure requires 20 minutes before the first field can be observed (t20 min). F)
822 Measure of the ability of LF82 to form microcolonies as a function of red TIMER
823 fluorescence at t20 min of the experiment are presented in E; areas of microcolonies are
824 expressed in pixels²;

825

826 **Figure 5.** A) Proportions of LF82, K12 and LF82 deletion mutants that were tolerant to a
827 3-h ciprofloxacin challenge following a 1 h or 24 h intracellular growth period within
828 THP1 macrophages. Values represent the average of 3 to 7 experiments. Data were
829 analyzed using a Student's *t* test to determine differences compared with WT LF82. **P* <
830 0.05. B) Measure of the proportions of LF82 *lexA ind*, *recA*, *sula*, *dksA*, *dksA lexAind*-,
831 *dksA recA* mutants that were tolerant to 3 h of cefotaxim challenge after 1 hour of
832 macrophage infection. The 3 hour time point was below detection limit for the *dksA recA*

833 mutant because of the poor viability of the mutant in macrophages. Cefotaxime only kills
834 growing bacteria; therefore we resuspended LF82 in LB after macrophage lysis. Under
835 these conditions, we did not observe the plateau observed for persisters to
836 ciprofloxacin, suggesting that tolerant rather than persister LF82 were measured. C)
837 Same as in B but with 20 h of macrophage infection. Values represent the average of 3 to
838 7 experiments. Data were analyzed using a Student's *t* test to determine differences
839 compared with WT LF82. **P* < 0.05. D) Imaging of the FD for the *relA spoT* and *recA*
840 mutants. Imaging at 24 h P.I. at an MOI 100x. Data represent the % of replicative and
841 non-growing LF82; a total of 300 bacteria were counted. E) Percentage of the LF82
842 population presenting a high, mid or low level of red TIMER fluorescence at 18 h P.I. of
843 macrophages. *recA*, *lexAind-*, *sulA* and *dksA* mutants were tested. F) Live and dead assay
844 performed 1h and 18h post infection, in the LF82, LF82*recA*, LF82*lexAind-*, LF82*sulA*,
845 LF82*relAspoT* and LF82*dksA* strains

846
847 **Figure 6.** A) Model of infection of THP1 macrophages by LF82, describing the processes
848 of net growth, switch to persistence and stress-induced death as explained in the text.
849 Part of the cells that enter the macrophage die at the onset of the infection ($t=0$). During
850 lag phase ($0 < t < \lambda$), death either exactly compensates birth or, in the mutant lacking the
851 stringent response, results in a negative net growth rate $-\delta_1$. Later in the infection, the
852 net growth rate β is positive. Death rate due to stress accumulation (yellow bar) is
853 negligible in the early stages of infection and becomes particularly important at late time
854 points. Bacteria switch to a persistent state at a rate k_p independent of the growth stage.
855 B) Experimental measures of the infection kinetics (CFUs from 5 replicate experiments,
856 circles; persister fractions, stars) collected over 24h for LF82, *E. coli* K12 and LF82 *dksA*
857 and the best fitting parameters (Supplementary text Table 1) of model eq. (1)
858 (Methods). Continuous lines represent total number of bacteria (B+P, continuous line)
859 and persisters (P, dotted line). Vertical lines indicate the duration λ of lag phase. C)
860 Projected changes in infection dynamics for 'virtual mutants' LF82*, obtained by varying
861 k_p , λ and d_{max} – the parameters that quantitatively differ between LF82 and *E. coli* K12 –
862 around the LF82 best fit solution (black line); coloured lines correspond to parameter
863 values within the indicated interval.

864
865 **Figure 7: Schematics of LF82 infection dynamics in macrophage phagolysosomes.**

866 Upon phagocytosis both replicative (green FtsZ ring) or stationary phase (brown) LF82
867 detect a signal, perhaps nutrient depletion, that led to stringent response activation. This
868 activates a first phenotypic switch toward a non replicating state (orange) that protects
869 LF82 from dying because of initial stress burst. Among these non replicating LF82
870 persisters are formed. After this lag phase, a second switch is required to initiate few
871 rounds of replication. The timing and perhaps the frequency of switching from lag phase
872 to replicative phase differentiate LF82 from our control commensal strain. We have not
873 yet identified LF82 specific determinants that allow this switch. Subsequent replication
874 rounds are dependent on the DNA repair machinery. A third switch, linked to the
875 increasing stress or lesions, is turned on in a portion of the replicative population to
876 form new non growers and persisters. The SOS response might also be playing a role at
877 this stage.

878

879

880

881

882 **Legend of the supplementary figures**

883

884 **Supplementary Figure S1.** A) Growth curves of LF82 and K12 (C600) in LB medium at
885 pH 7.4 (blue) and in the presence of SHX (15 mg/ml), SHX (7 mg/ml), EDTA (70 mM) or
886 in LB at pH 4.7 and LB at pH 4.7 in the presence of EDTA (70 mM). B) Chemicals or a pH
887 shift were applied at 160 min. B) same as in A with addition of the antibiotics
888 ciprofloxacin (24 ng/ml) or cefotaxim (800 ng/ml). Data are the mean of 3 technical
889 replicates.

890

891 **Supplementary Figure S2.** A) Live and dead assay performed in situ on infected
892 macrophages and after macrophage lysis. For in situ experiments a very weak
893 propidium iodide (PI) labeling is observed on putative dead LF82. By contrast strong PI
894 labeling is observed after macrophage lysis. B) Measure of the speed of disappearance
895 after phagocytosis by macrophages of heat-killed LF82. LF82 were killed by 15 min
896 incubation at 60°C and subsequently labeled with propidium iodide. Labeled dead LF82
897 were incubated with macrophage at an MOI of 100. Imaging was performed at 1h, 2h,
898 3h and 24h post infection. SYTO-9 was used to reveal macrophage and eventual live
899 bacteria. The number of dead LF82 per macrophage was measured at each time points.
900 Data are average of 3 experiments.

901

902 **Supplementary Figure S3.** A) Measure of the resistance to MMC of LF82, LF82 *recA*,
903 LF82 *lexAind-*, MG1655, MG1655 *recA* and MG1655 *lexAind-*. B) Measure of the tolerance
904 to cefotaxim of LF82 and LF82 *recA*, LF82 *lexAind-*, LF82 *sulA* grown in LB medium to an
905 OD of 0.2. C) Induction of tolerance to cefotaxim by pretreatment with a subinhibitory
906 dose of ciprofloxacin (24 ng/ml). The data represent the ratio of the number of bacteria
907 that were tolerant to 3 h of cefotaxim in the presence or absence of ciprofloxacin.

908

909 **Supplementary Figure S4.** A) Growth curve of LF82 pFC6Gi in LB at 37°C. Colored
910 diamonds represent the sampling times analyzed by fluorescence microscopy in the
911 panel B. B) Distribution of GFP fluorescence in the growing population of LF82; GFP
912 fluorescence is expressed as the number of generations (each generation corresponds to
913 a 2-fold decrease in GFP fluorescence compared with the average fluorescence of the
914 fully induced population at t₀). C) Distribution of GFP fluorescence in the population of

915 LF82-infecting macrophages. Fluorescence was measured for individual bacteria or
916 small bacterial clusters after macrophage fixation at 1 h, 6 h, 24 h and 48 h post-
917 infection. D) Distribution of the GFP fluorescence in the population of K12 bacteria
918 infecting macrophages. Fluorescence was measured for individual bacteria or small
919 bacterial clusters after macrophage fixation at 1 h and 24 h post-infection.

920

921 **Supplementary Figure S5.** A) Scatter plot of green versus red TIMER fluorescence
922 measured for exponentially growing LF82 (green) and for a culture that had reached
923 stationary phase (red). B) Distribution of the red TIMER fluorescence measured for
924 exponentially growing LF82 (green) and stationary phase LF82 (red) at 4 h and 18 h
925 post-infection. Curves represent the normal fit of the data. The middle peak height for
926 exponential and stationary cultures was used to respectively define the fast-mid and
927 mid-slow borders of the boxes.

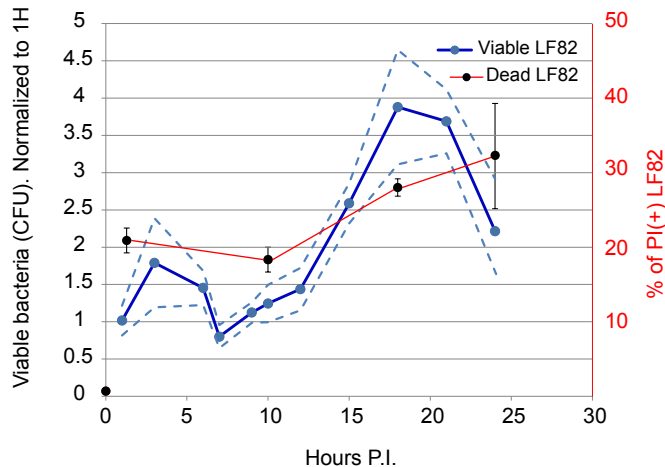
928

929

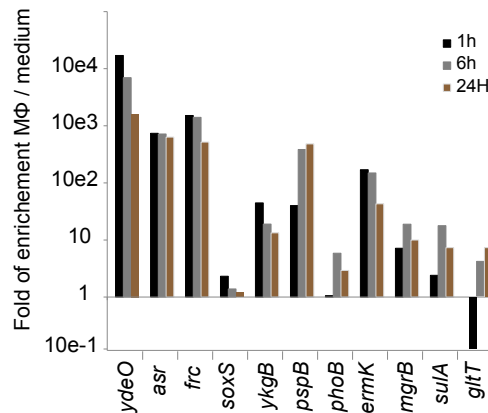
930

931

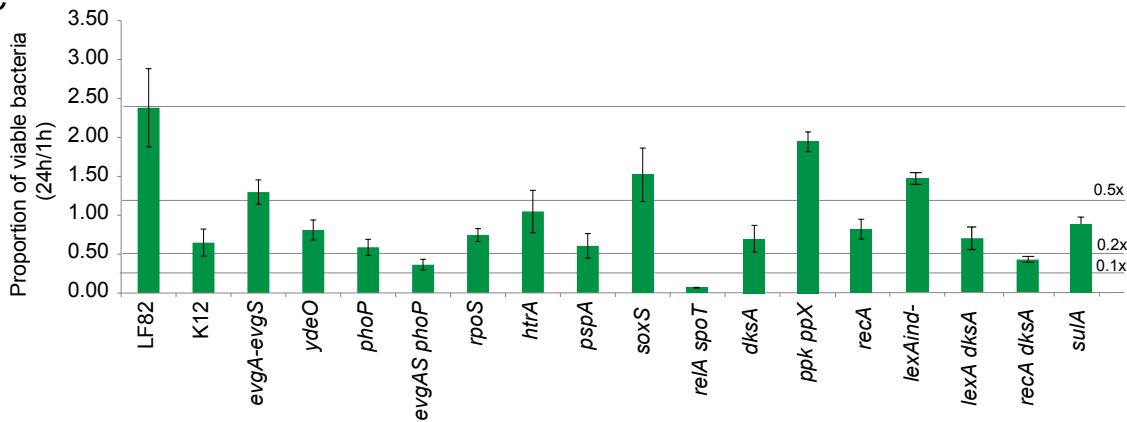
A



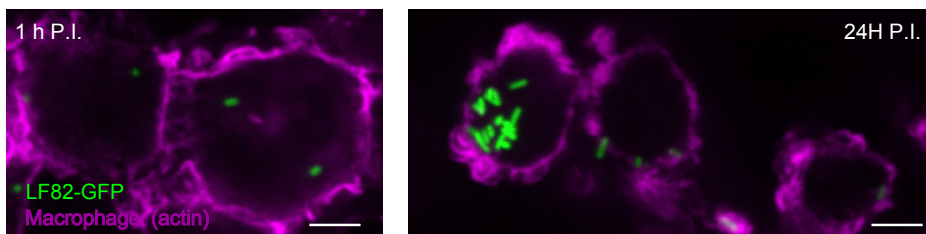
B



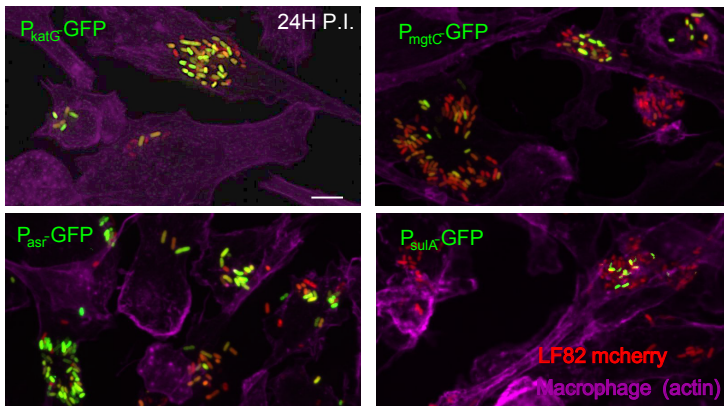
C



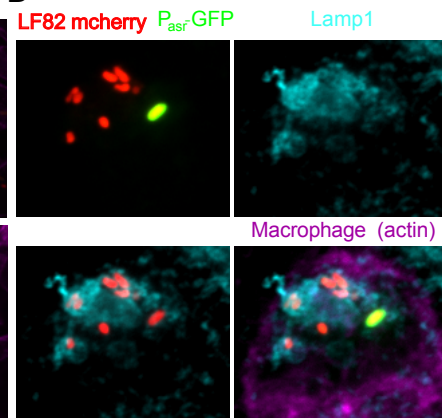
A



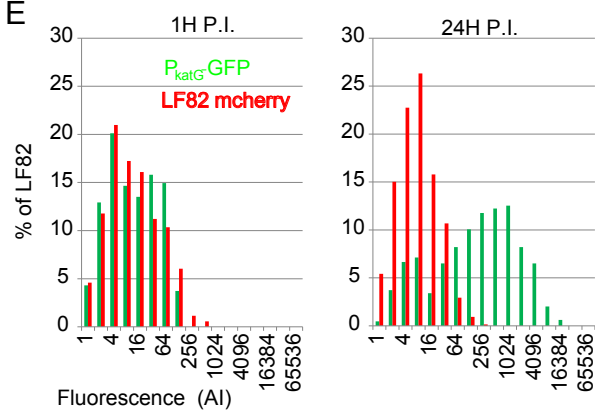
C



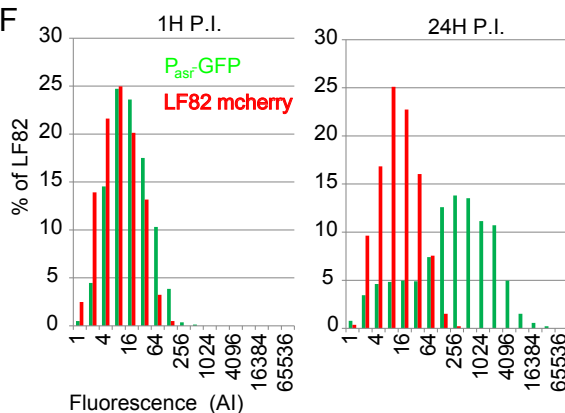
D



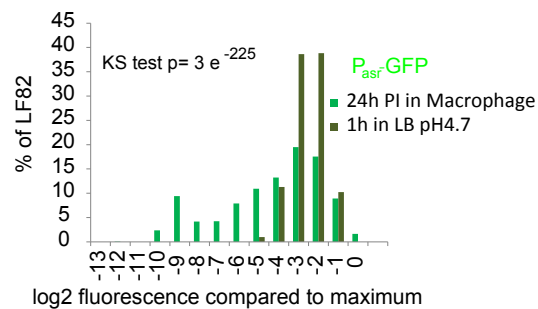
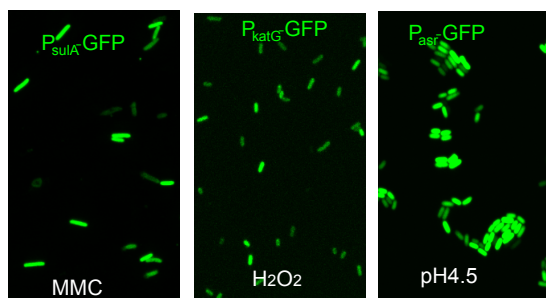
E

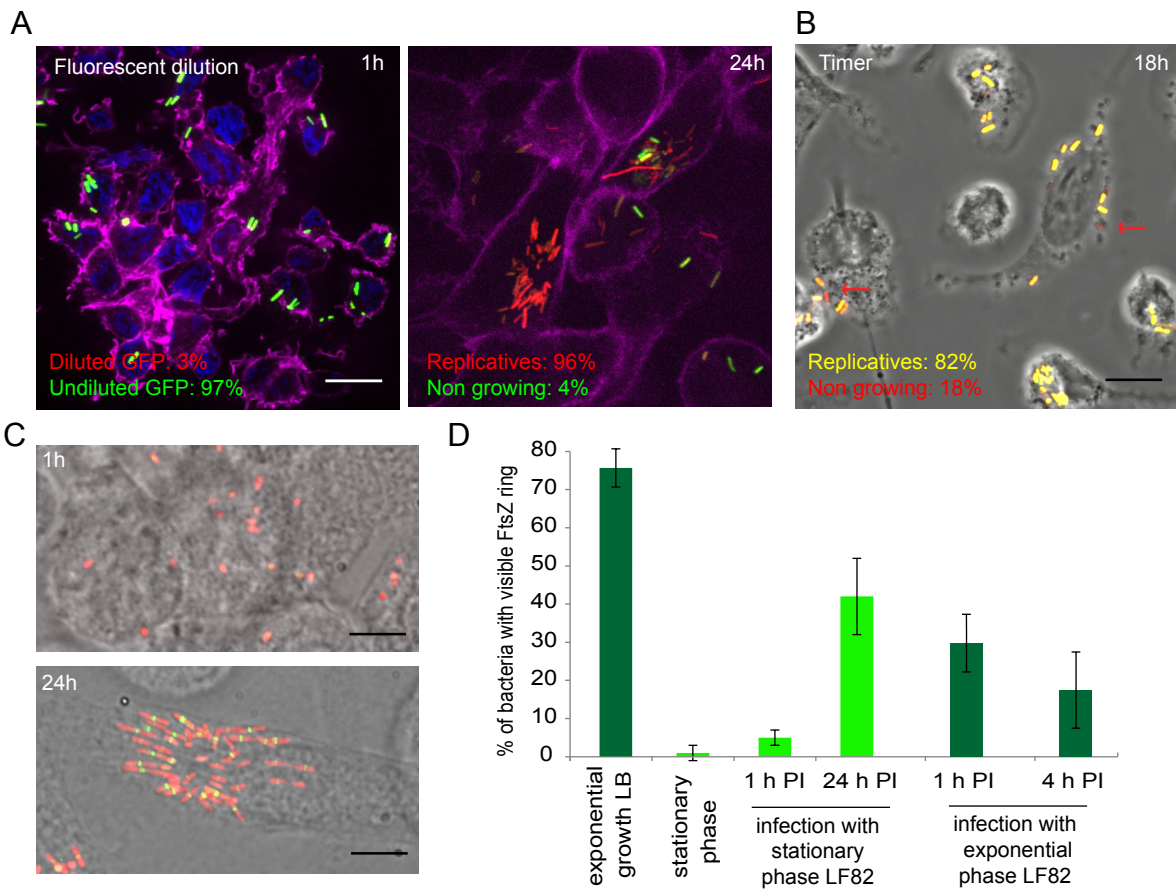


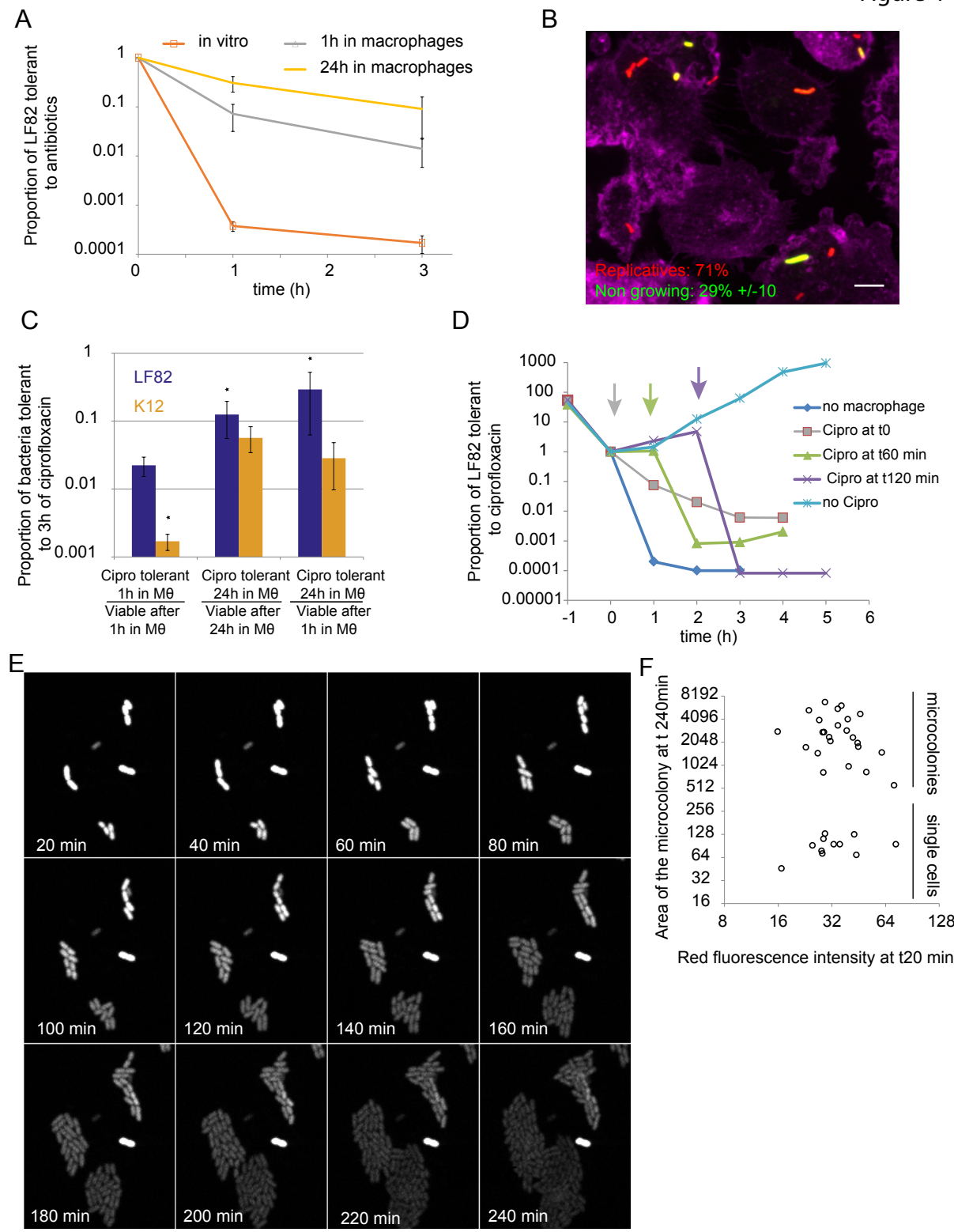
F

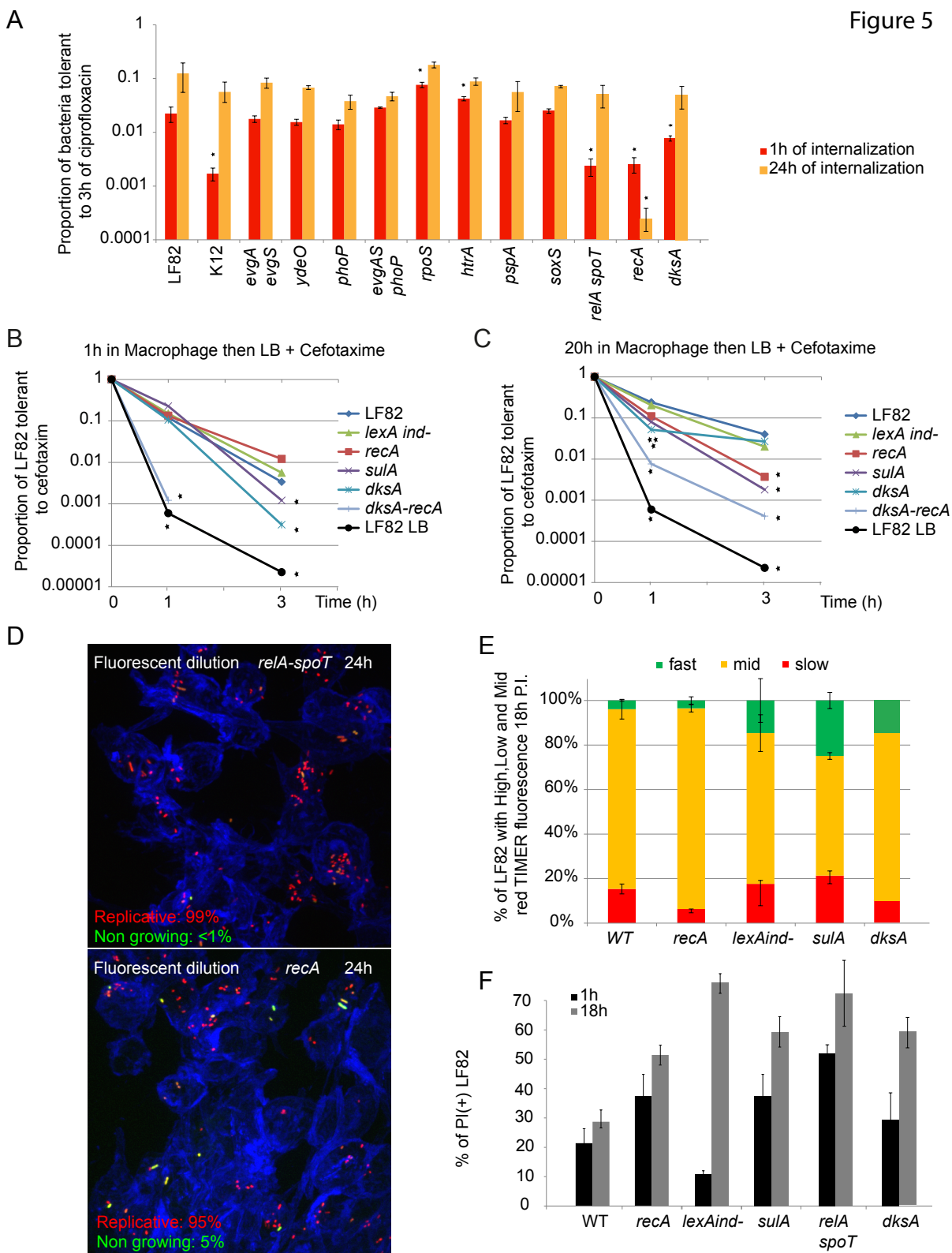


G

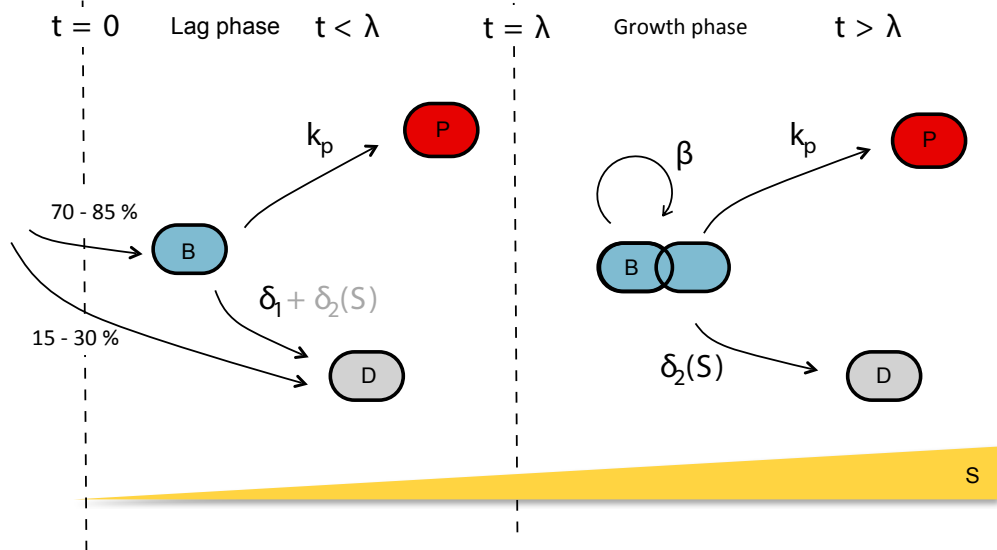




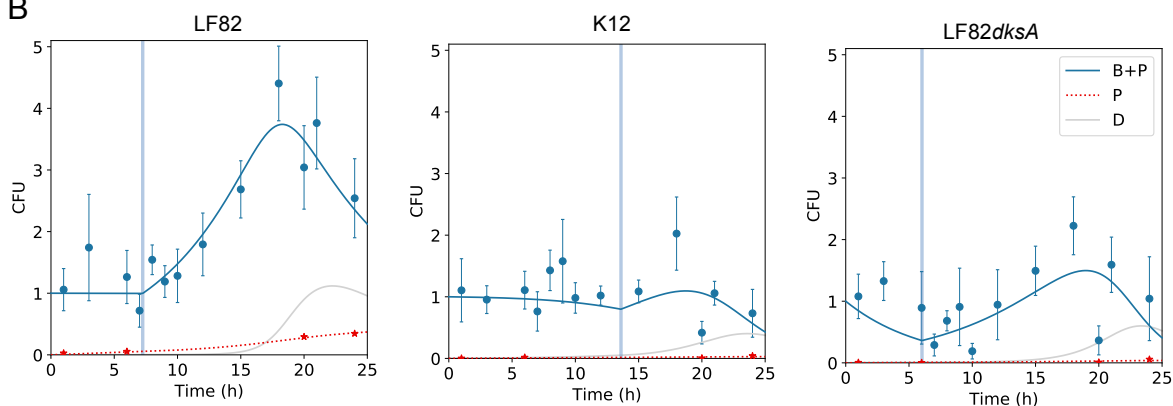




A



B



C

